Biosensors and Bioelectronics 105 (2018) 14–21

Contents lists available at ScienceDirect

Biosensors and Bioelectronics

journal homepage: www.elsevier.com/locate/bios

Ultrasensitive electrochemical immuno-sensing platform based on gold nanoparticles triggering chlorpyrifos detection in fruits and vegetables

Anita Talan[a], Annu Mishra[b], Sergei A. Eremin[c,d], Jagriti Narang[b], Ashok Kumar[e], Sonu Gandhi[a,*]

[a] Amity Institute of Biotechnology, Amity University, Sector-125, Noida, 201313, India
[b] Amity Institute of Nanotechnology, Amity University, Sector-125, Noida, 201313, India
[c] M.V. Lomonosov Moscow State University, Faculty of Chemistry, Department of Chemical Enzymology, Leninsky Gory 1, 119991 Moscow, Russia
[d] A.N. Bach Institute of Biochemistry of the Russian Academy of Sciences, Leninsky prospect 33, 119071 Moscow, Russia
[e] CSIR-Institute of Genomics and Integrative Biology, Mall Road, Delhi 110007, India

ARTICLE INFO

Keywords:
Fluorine doped tin-oxide
Nanosensor
Chlorpyrifos
Gold nanoparticles
Antibodies
Immunoassay

ABSTRACT

Chlorpyrifos (chl) is an organophosphate pesticide extensively used in agriculture and highly toxic for human health. Fluorine doped tin-oxide (FTO) based electrochemical nanosensor was developed for chlorpyrifos detection with gold nanoparticles (AuNPs) and anti-chlorpyrifos antibodies (chl-Ab). AuNPs provides high electrical conductivity and specific resistivity, thus increases the sensitivity of immunoassay. High electrical conductivity of AuNPs reveals that it promotes the redox reaction for better cyclic voltammetry. Based on the intrinsic conductive properties of FTO-AuNPs complex, chl-Ab was immobilized onto AuNPs surface. Under optimized conditions, the proposed FTO based nanosensor exhibited high sensitivity and stable response for the detection of chlorpyrifos, ranging from 1 fM to 1 μM with limit of detection (LOD) up to 10 fM. The FTO-AuNPs sensor was successfully employed for the detection of chlorpyrifos in standard as well in real samples up to 10 nM for apple and cabbage, 50 nM for pomegranate. The proposed FTO-AuNPs nanosensor can be used as a quantitative tool for rapid, on-site detection of chlorpyrifos traces in real samples when miniaturized due to its excellent stability, sensitivity, and simplicity.

1. Introduction

Chlorpyrifos (O, O-diethyl-O-3, 5, 6-trichloro-2-pyridylphosphorothioate) is an organophosphate, a broad spectrum pesticide widelyused in agriculture for the prevention and control of harmful insects and mites on various field crops like fruits, vegetables, cotton, and tea etc. (Chen et al., 2015). Chlorpyrifos is one of the largest used pesticides globally and it enters the food chain and causing harmful effects in animals and humans (Suri et al., 2009). Prolonged exposure of pesticide causes chronic diseases such as cancer, reproductive disorders, neurological disorders, allergic reactions, and most importantly neurodevelopmental impairment in growing children (Chen et al., 2015; Seiber and Kleinschmidt, 2011).

Till date, many qualitative as well as quantitative techniques have been developed for pesticide detection, such as chromatographic techniques e.g. gas chromatography (GC) and high performance liquid chromatography (HPLC) (Hercegova et al., 2007; Suri et al., 2008; Guan et al., 2010; Alamgir Zaman Chowdhury et al., 2013; Zalat et al., 2014; Zhao et al., 2014). These are instrument based techniques that provides high sensitivity, but poses many drawbacks such as time consuming, costly, not amenable to on-site application, and requires trained personnel. Enzyme linked immunosorbant assay (ELISA) employs the reaction of antigen (Ag) and antibody (Ab) that is quick and simple, but it causes interference due to the presense of organic solvent or matrix components (Gandhi et al., 2009; Funari et al., 2013, 2015). Compared to these methods, electrochemical biosensors have several advantages such as fast response, high sensitivity, low cost, and on-site detection that makes electrochemical biosensors a promising alternative tool for rapid detection of pesticides, glucose, adulteration, cancer, and narcotic drugs (Wijaya et al., 2010; Sharma et al., 2010; Thakur et al., 2011; Jiao et al., 2016; Xiang and Tang, 2017; Li et al., 2015; Zhang et al., 2017; Ji et al., 2017; Guohua et al, 2017; Lu et al., 2017; Hui et al., 2016; Jiaojiao et al., 2015; Hui et al., 2015; Zhu, 2015). Various analytical methods have been developed for chlorpyrifos detection and analyzed by change in fluorescence intensity (Azab et al., 2015). Enzyme based electrochemical biosensor have been developed for a class of pesticides. Achetylcholinesterase (AChE) inhibits AChE and affects the signalling pathways, that form the basis for the detection of AChE (Qu et al., 2010). Utilization of nanomaterials result in improved sensitivity and specificity for signal amplification. Gold

* Corresponding author.
E-mail addresses: sgandhi@amity.edu, sonugandhi@gmail.com (S. Gandhi).

https://doi.org/10.1016/j.bios.2018.01.013
Received 16 November 2017; Received in revised form 3 January 2018; Accepted 8 January 2018
Available online 09 January 2018
0956-5663/

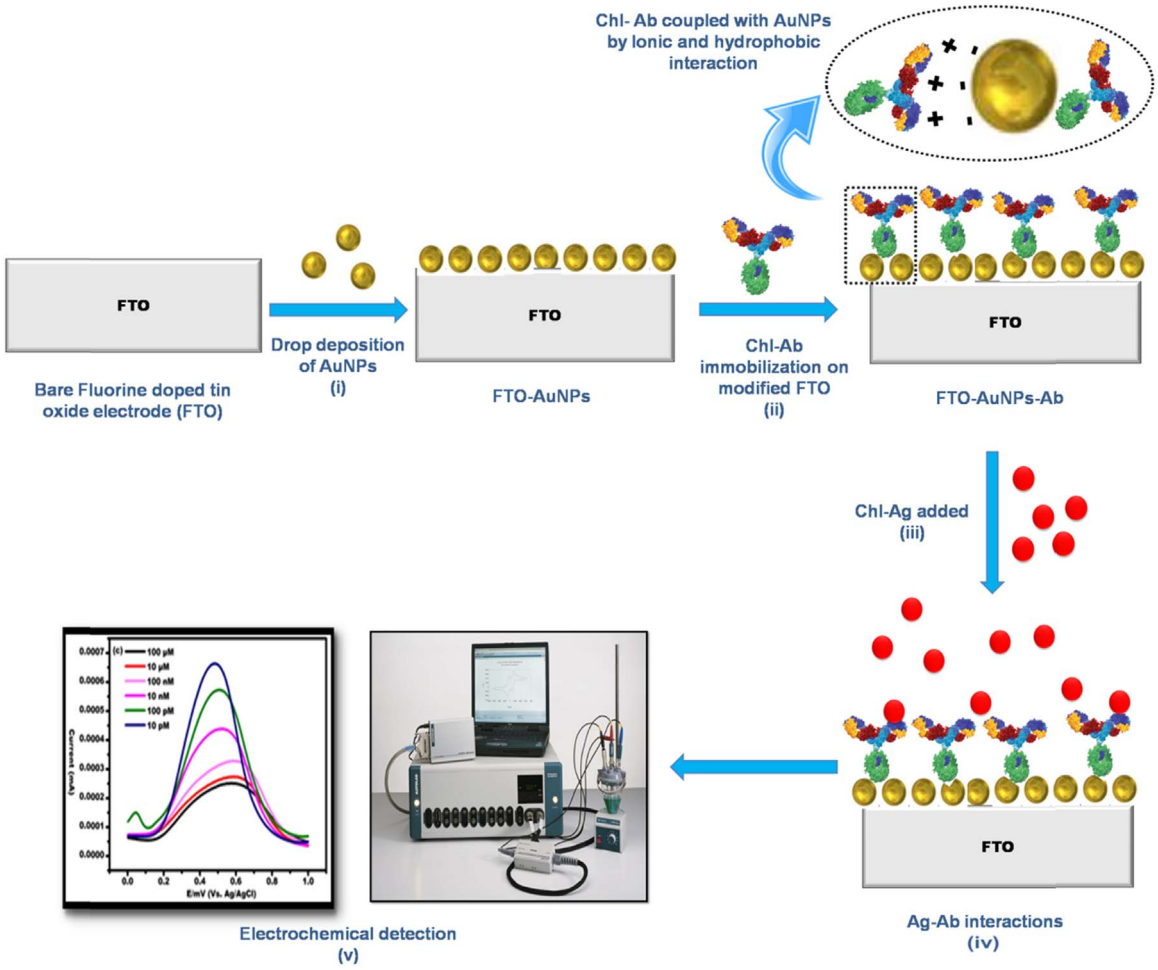

Scheme 1. Schematic representation of the fabrication process of FTO-AuNPs-chl-Ab where (i) bare FTO electrode was used and (ii) AuNPs were drop casted on its surface. Anti-chl-Abs were immobilized on FTO-AuNPs modified surface and (iv) Ag-Ab interactions were analyzed by (v) Electrochemical detection.

nanoparticles (AuNPs) were used to develop colorimetric sensor due to its optical and surface plasmon resonance properties. Aptamers specific for chlorpyrifos were labelled with cysteamine stabilized gold nanoparticles (CS-AuNPs) (Luo et al., 2015). Tang et al. used quantum dot based DNA aptamer coupled with capillary electrophoresis for chlorpyrifos detection in pure water and fresh apples (Tang et al., 2016). On the other side, immunosensors are highly sensitive and specific due to antigen-antibody interactions, and widely accepted for pesticide detection (Suri et al., 2009). Multiwalled carbon nanotubes (MWCNT) based portable immunosensor was developed for the detection of chlorpyrifos (Sun et al., 2012a, 2012b; Ding et al., 2014).

The aim of the present work was to develop a sensitive, specific and economic nanosensor for the detection of chlorpyrifos pesticide. For this, novel fluorine doped tin oxide electrode (FTO) nanosensor was developed using AuNPs. Here, AuNPs were preferred because of its high conductivity, stability, biocompatibility, and size related electronic properties. AuNPs immobilized on the surface of FTO that served as a bridge for the signal amplification via Ag-Ab interaction. AuNPs also provide the platform for immobilization of anti-chlorpyrifos antibody (chl-Ab). The FTO coated glass plate was mainly used because fabrication of AuNPs on FTO electrode is a facile approach as it provides high electrical conductivity, and cost effective. The FTO and AuNPs provides amplification of sensing signal which lead to high sensitivity of the developed platform while use of antibody provided specificity to the sensor. Based on the synergistic effects of FTO and AuNPs, fabricated nanosensor provided high specificity and sensitivity for the detection of chlorpyrifos in fruits and vegetables.

2. Materials and methods

2.1. Reagents

Chlorpyrifos (chl), chlorpyrifos antibody (chl-Ab), chloroauric acid ($HAuCl_4$), sodium hydrogen phosphate (Na_2HPO_4), potassium dihydrogen phosphate (KH_2PO_4), sodium citrate tribasic dehydrate ($C_6H_5Na_3O_7{\cdot}2H_2O$), potassium chloride (KCl)), potassium ferrocynaide ($K_4Fe(CN)_6{\cdot}3H_2O$), potassium ferricyanide ($C_6N_6FeK_3$), FTO-electrode were purchased from Sigma (India). chl-Ab was purchased from creative diagnostics, USA. All other reagents used were of high quality analytical grade unless otherwise stated. All solutions were prepared using double distilled water (DDW).

2.2. Apparatus

The Uv–vis spectrum was taken with Uv–vis spectrophotometer (S-925) from Systonic, India. Cyclic voltammetry (CV) and differential pulse voltammetry (DPV) measurements were performed with Autolab-PGSTAT-10, Eco Chemie, and Utrecht, Netherlands driven by Nova software. The commercially available fluorine doped tin-oxide electrode (working dimensions were 10 mm and 30 mm) was purchased from Sigma Aldrich (India). All experiments were performed with three-electrode system at room temperature (RT) at 25 ± 1 °C. DLS, was done with Nicomp 380ZLS (Particle Sizing Systems, Port Richey, FL, USA) particle sizing system equipped with green laser excitation source operating at 532 nm/50 mW. EDAX analysis and transmission electron

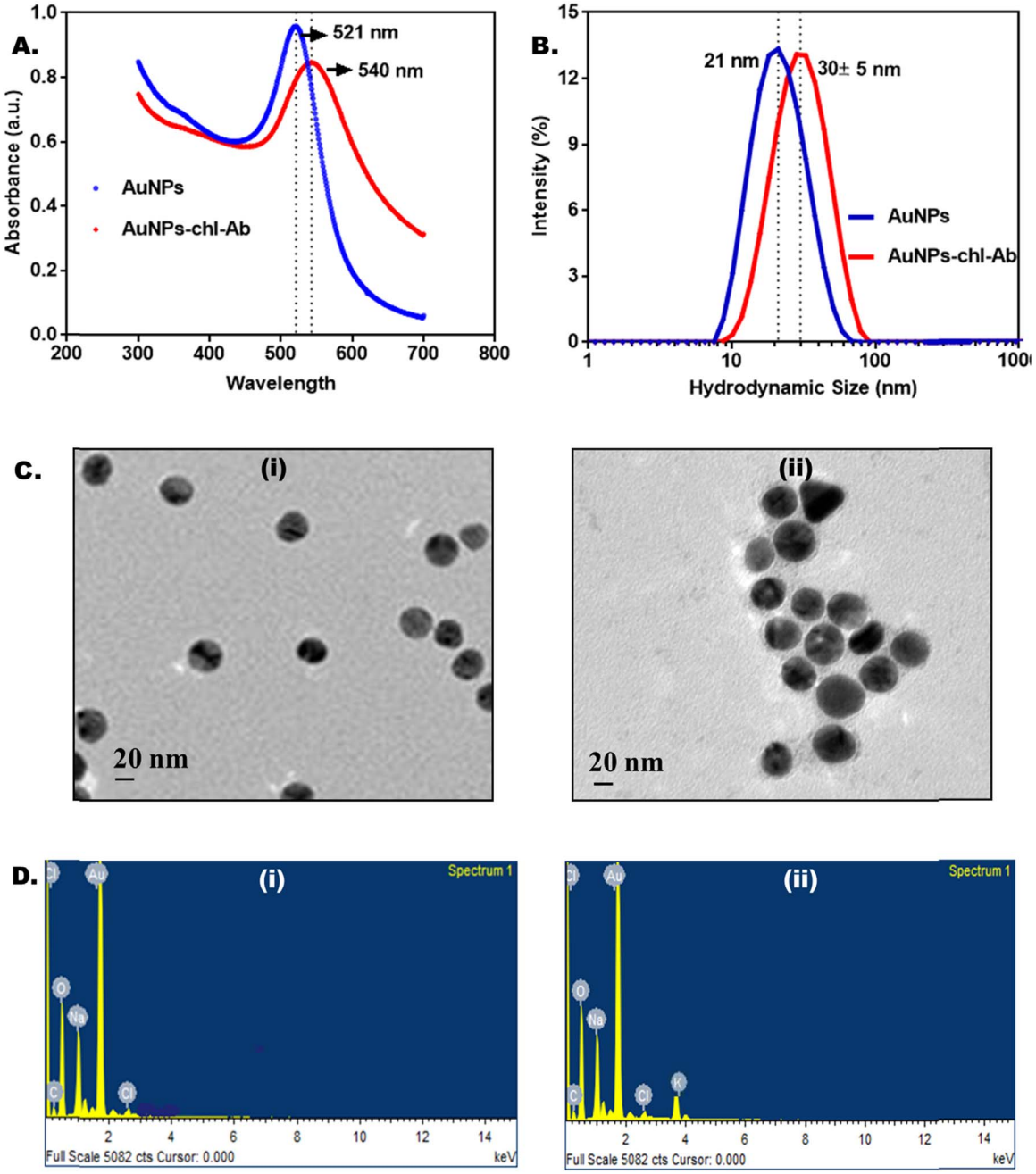

Fig. 1. UV–vis spectra (A) at 521 nm showed the synthesis of AuNPs and change in peak from 521 nm to 540 nm confirmed the binding of chl-Ab to AuNPs (B) DLS spectra of AuNPs and AuNPs-chl-Ab. The hydrodynamic diameter of AuNPs was approximately 21 ± 5 nm while after binding of chl-Ab the resonance peak was shifted to 30 ± 5 nm. (C) TEM images of AuNPs and AuNPs-Ab (C-i) the monodispersed AuNPs showed the size of 20 ± 5 nm (C-ii) AuNPs-chl-Ab showed the encircled area of chl-Ab coated over gold nanoparticles (AuNPs). (D) EDAX spectra of AuNPs (D-i) and chl-Ab-AuNPs (D-ii) showed the presence of Au that confirmed the synthesis of AuNPs and peak of K (nitrogen) confirmed the binding of chl-Ab to AuNPs.

microscopy (TEM) was done with JEOL-JEN 2010 operated at an accelerating voltage of 200 kV.

2.3. Synthesis of AuNPs and its labelling with chl- Abs

Frens methodology (Frens, 1973) was followed to synthesize AuNPs. 200 mL solution of 0.01% gold chloride was heated. To this, trisodium citrate (4 mL; 1% w/v) solution was added and continues to boil until turned into wine red colour. To prepare AuNPs-chl-Ab conjugate, chl-Ab (90 µg) was added dropwise to colloidal gold chloride solution (1 mL; 20 mM phosphate buffer, pH 7.5). The labelling was carried out overnight (O/N) at 4 °C and centrifuged at 10, 000 rpm for 35 min to remove unbound antibody. The pellet (AuNPs-chl-Ab) was resuspended in 20 mM phosphate buffer, pH 7.5 for further use.

2.4. Characterization of AuNPs and AuNPs-chl-Ab

The bio-reduction of Au(III) ions to Au° was observed using Uv–vis spectrophotometer. The absorption spectrum was acquired in the range of 200–800 nm with a step of 0.1 nm and scanning speed of 20 nm/s. The obtained spectrum was compared for AuNPs and AuNPs-chl-Ab. The concentration of AuNPs-chl-Ab was found to be 0.5 µg/mL.

The hydrodynamic diameter of AuNPs and AuNPs-chl-Ab was determined by DLS at a frequency of 200 kHz for photon counting, scattering angle was fixed at 90 °C, and temperature of the measured media was within 24 ± 2 °C. The hydrodynamic diameter of AuNPs and

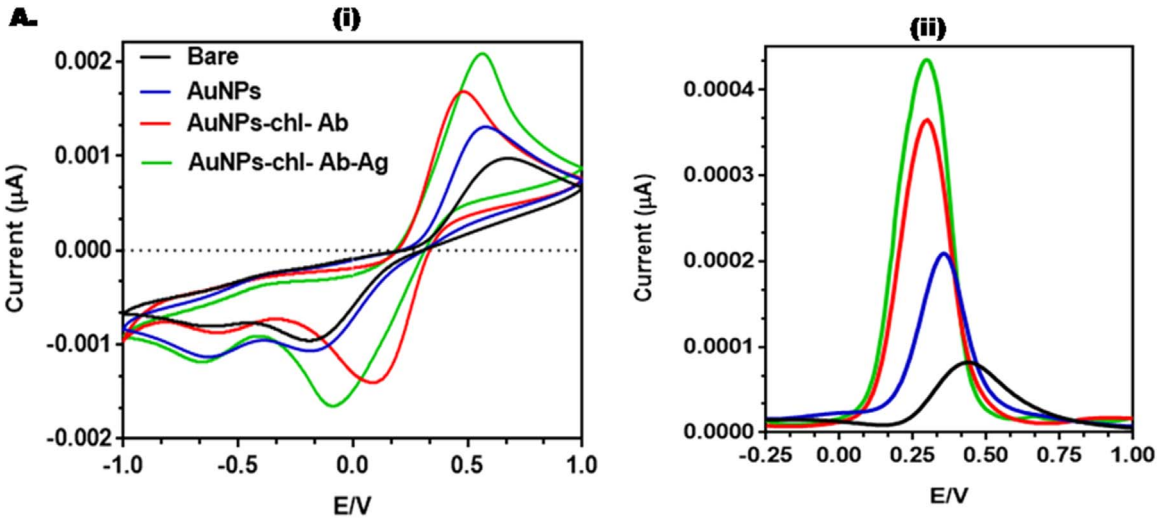

Fig. 2. (i) Electrode characterization (i) Cyclic voltammograms (CV) of FTO, FTO-AuNPs and FTO-AuNPs-chl-Ab electrode in the scanning potential range of −1.0 to 1.0 V in 0.1 M KCL with 5 mM $K_4Fe(CN)_6{\cdot}3H_2O$ and 5 mM $C_6N_6FeK_3$ buffer pH 7.5, at the scan rate 100 mV/s (ii) Differential pulse voltammogram (DPV) of FTO, FTO-AuNPs and FTO-AuNPs-chl-Ab electrode in the scanning potential range of 0–1.5 V in 0.1 M KCL with 5 mM $K_4Fe(CN)_6{\cdot}3H_2O$ and 5 mM $C_6N_6FeK_3$ buffer pH 7.5 at the scan rate of 100 mV/s.

AuNPs-chl-Ab was calculated based on Stokes–Einstein equation (Huang et al., 2014), considered water as continuous phase (water viscosity = 0.911–0.852 mPa/s, diffusion coefficient of AuNPs = 6.89 × 10^{-9} to 5.30 × 10^{-8} cm^2/s).

Morphology and size of AuNPs and AuNPs-chl-Ab (after negative staining) was analyzed by TEM. The sample deposited on carbon coated copper TEM grid was allowed to dry in air by placing a drop of solutions for few min before analysis. For EDAX analysis, AuNPs and AuNPs-chl-Ab solutions were air dried, drop coated on to carbon film, and tested for the presence of elements.

2.5. Fabrication of FTO-AuNPs-chl-Ab electrode

2.5.1. Preparation of electrode

The FTO electrode was washed thoroughly with DDW and air dried at RT. AuNPs (200 μL) were immobilized on FTO electrode and completely dried for 48 h at 4 °C followed by addition of chl-Ab (40 μL of 0.50 μg/mL) to immobilize for 24 h at 4 °C.

2.5.2. Electrochemical characterization of FTO-AuNPs-chl-Ab electrode

The electrochemical performance of FTO-AuNPs-chl-Ab electrode was carried out using cyclic voltammetry (CV) by sweeping the potential from −1.0 to 1.0 V in $K_3[Fe(CN)_6]/K_4[Fe(CN)_6]$ (1:1) solution containing 0.1 M KCl. Various parameters such as antibody concentration, scan rate, response time, pH and temperature were optimized in order to obtain maximum sensing signal. Various concentrations ranging from1 fM to 1 μM of chl-Ag were prepared. Cross-reactivity of fabricated immunosensor was analyzed with 2,4-D (2, 4-dichlorophenoxyacetic acid) at similar concentration used for chl-Ag.

2.5.3. Application of fabricated biosensor in real samples

The sensitivity, specificity and applicability were also evaluated in fruits and vegetables (apple, pomegranate and cabbage). 5 g of apple, pomegranate and cabbage was crushed separately using mortar-pestle and mixed in 5 mL of PBS, pH 7.5. After this, the sample was prepared andcentrifuged for 10 min at 10,000 rpm. 1 mL of real samples (apple, pomegranate and cabbage) was added directly onto FTO-AuNPs-chl-Ab electrode for the presence of chl pesticide.

3. Results and discussion

3.1. Design and principle of FTO nanosensor

Fabrication principle of proposed FTO nanosensor coupled with AuNPs and anti-chlorpyrifos antibodies (chl-Ab) is illustrated in Scheme 1. AuNPs immobilized on the surface of FTO served as a bridge for signal amplification due to its high electrical conductivity. Furthermore, AuNPs also provide the platform for immobilization of chl-Ab by ionic or hydrophobic interactions. The physiosorption of AuNPs was done in order to provide the homogenous layer on the surface of FTO electrode for high electrical conductivity. Chl-Ab were immobilized on AuNPs fabricated FTO electrode, followed by addition of specific Ag for chlorpyrifos detection that produced significant changes in current. The designed sensor effectively combined the advantageous features of FTO electrode, AuNPs and high specificity of chl-Ab that eventually produced fast response with very low limit of detection.

3.2. Characterization of FTO nanosensor

Uv–Vis spectra (Fig. 1A) were recorded in the range of 200–800 nm for AuNPs and AuNPs-chl-Ab. A peak of AuNPs at was observed 521 nm due to its surface plasmon properties while broadened peak and red shift at 540 nm confirmed the binding of AuNPs with chl-Ab. The change in hydrodynamic diameter was observed from 21 nm (AuNPs) to 30 nm (chl-Ab to AuNPs) that reconfirmed the binding as shown in Fig. 1B.

The confirmation of size and morphology of AuNPs and AuNPs-chl-Ab was done by TEM as depicted in Fig. 1C (i) and C (ii) respectively. AuNPs present in narrow diameter distribution and in monodispersed state with average diameter of 20 ± 5 nm. Fig. 1C (ii) showed the binding of AuNPs-chl-Ab that can be observed by deposition of proteinaceous substance (chl-Ab) on the surface of AuNPs.

Further detailed elemental analysis was done by EDAX to confirm the presence of AuNPs (Fig. 1D (i)) and AuNPs-chl-Ab (Fig. 1D (ii)). The EDAX spectra proved further the confirmation of labelling by presence of peak of Au in AuNPs and K (for N) in case of AuNPs-chl-Ab. The above results indicated that AuNPs were successfully labelled with chl-Abs and can be further utilized for immobilization on to FTO electrode.

3.3. Electrochemical characterization of nanosensor

Cyclic voltammograms (CV) with ferro/ferricyanide redox probe

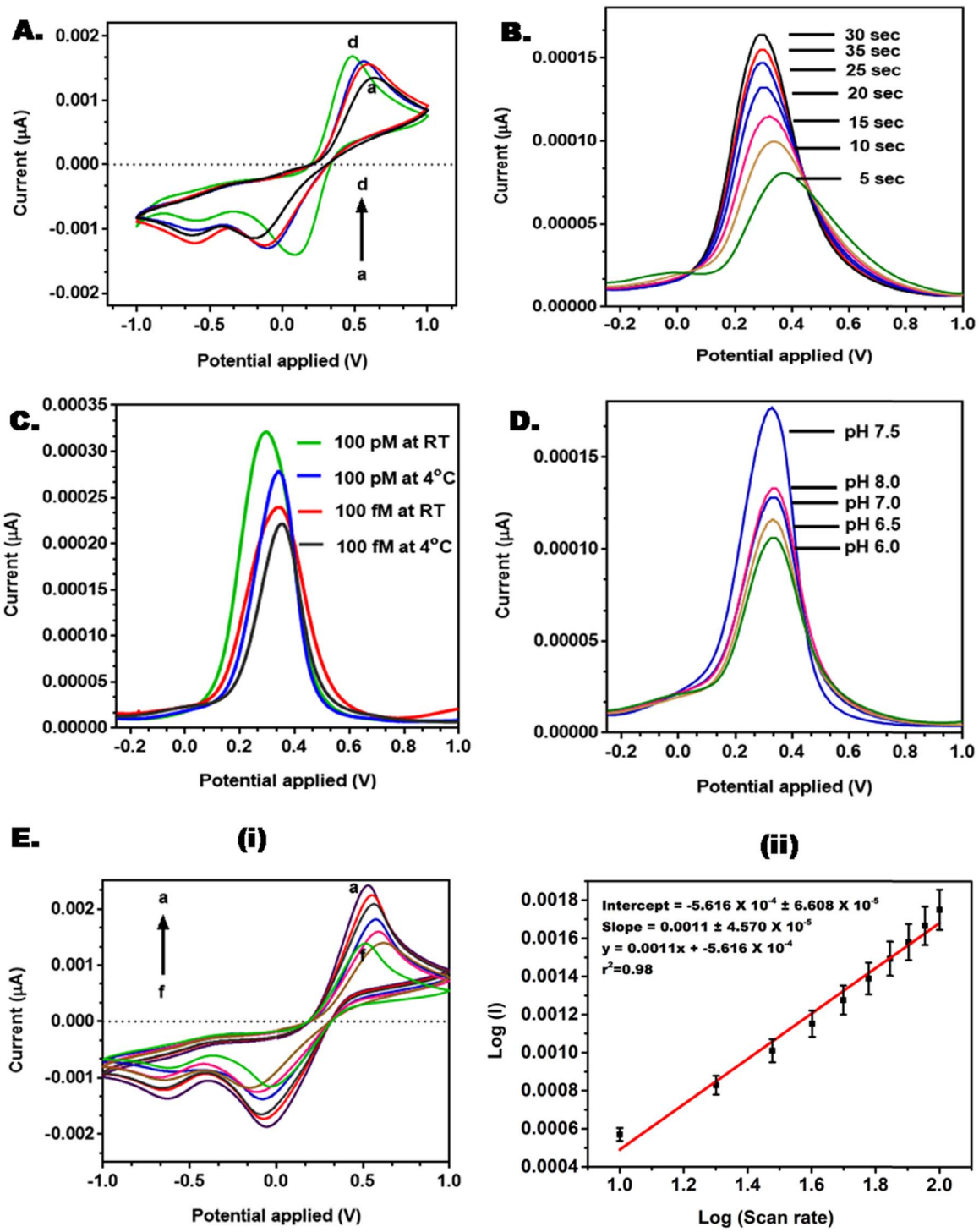

Fig. 3. (A) CV for chl-Ab concentrations ranging from (a) 0.25 (b) 0.50 (c) 0.75, and (d) 1 μg/mL (in the scanning potential range of 0–1.5 V; (B) DPV of FTO-AuNPs-chl-Ab at different response time ranging from 5 to 35 s in the same buffer as in Fig. 3A; (C) DPV at FTO-AuNPs-chl-Ab at room temperature (RT) and 4 °C; (D) DPV at different pH ranging from 6.0 to 8.0; (E) CV for (E-i) different scan rates was optimized from 10 to 100 mV/s; (E-ii) Calibration plot between log of the various scan rates. The buffer used for all the optimization studies was 0.1 M KCL with 5 mM $K_4Fe(CN)_6{\cdot}3H_2O$ and 5 mM $C_6N_6FeK_3$ buffer pH 7.5.

was utilized for the characterization of bare FTO, AuNPs and AuNPs-chl-Ab modified electrode (Fig. 2). The bare FTO electrode showed static response to redox probe (solid curve) in comparison with electrode modified with AuNPs. This may be due to the fact of high conductivity of AuNPs that accelerate the electron transfer rate (Tey et al., 2010). Further high surface area of AuNPs provides additional benefits to the sensing interface. A clear amplified pair of redox peaks for the ferro/ferricyanide probe was observed with AuNPs-modified FTO electrode, which was due to increased permeability enabling ferrocyanide to diffuse through gold nanoparticles towards electrode surface. The significant difference was observed in voltammetric signal when chl-Ab coupled with AuNPs because the captured antibody blocked the smooth diffusion of ferricyanide towards the electrode surface. This might be due to the fact that antibody insulated the conductive interface which makes difficulty in transportation of electrons. Results of CV (Fig. 2A(i)) were also confirmed with differential pulse voltammogram

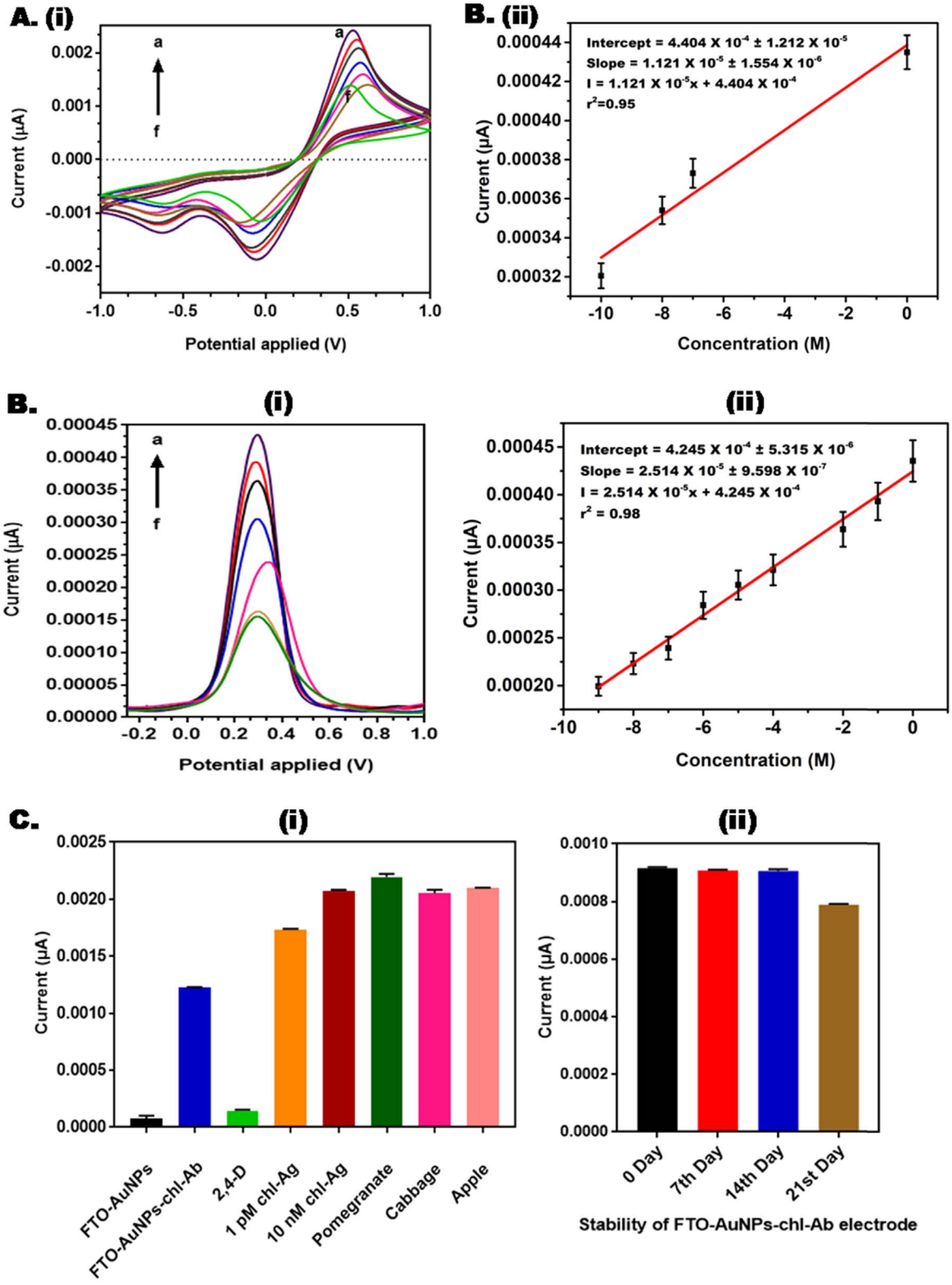

Fig. 4. (A-i) CV for different antigen concentrations (chl-Ag) ranging from (i) 1 fM (ii) 10 fM (iii) 100 fM (iv) 1 pM (v) 10 pM (vi) 10 nM (vii) 100 nM (viii) 1 μM (in the scanning potential range of 0 V to 1.5; (A-ii) Calibration plot between log of the various concentrations of chl-Ag and peak current; (B-i) DPV of the same as shown in this figure. A-i; (B-ii) Calibration plot of the same; (C-i) Relative peak current value of DPV after binding of FTO-AuNPS-chl-Ab with chl-Ag in real samples (apple, pomegranate and cabbage). Cross reactivity study was done with 2,4-D on FTO-AuNPs-chl-Ab electrode where negative control (FTO-AuNPselectrode) and positive control (FTO-AuNPs-chl-Ab). (C-ii) Current response of the FTO-AuNPs-chl-Ab electrode was evaluated at 0th day, 7th day, 14th day and 21st day to confirm the stability. Chl-Ab was used at 0.50 μg/mL in scanning potential range of −1.0 to 1.0 V in 0.1 M KCL with 5 mM $K_4Fe(CN)_6{\cdot}3H_2O$ and 5 mM $C_6N_6FeK_3$ buffer pH 7.5, at the scan rate 100 mV/s.

Table 1
Comparison of various electrochemical sensors developed for the detection of chlorpyrifos.

Electrode	Limit of Detection (LOD)	Linear Range	Response time	References
AChE/PAMAN-Au/CNTs	4.0×10^{-9} M	4.8×10^{-9} M to 0.9×10^{-7} M	–	Qu et al. (2010)
AChE-TCNQ- PVA-SbQ	10^{-9} to 8×10^{-9} M	–	–	Nunes et al. (2004)
MWCNTs-THI-CHIT/GCE	0.046 ng/mL	0.1 to 1.0 × 105 ng/mL	25 min	Sun et al. (2012a, 2012b)
GC-MWCNT-CoPc	5.46 ± 0.02 nmol/L	0.33–6.61 μmol/L	–	Moraes et al. (2009)
AChE/Au/Chi	0.001 μg/mL	0.004–24 μg/mL	10 min	Li et al. (2010)
AChE/PB-CHIT/GCE	3 nM	0.01–0.4 μM	300 s	Song et al. (2011)
AChE-CdS-G-CHIT-GCE	0.7 ng/mL	2 ng/mL to 2 g/mL	2 min	Wang et al. (2011)
Au/ssDNA-SWCNT/PANI/AChE	1×10^{-12} M	1.0×10^{-11} to 1.0×10^{-6} M	15 min	Viswanathan et al. (2009)
[BMIM][BF4]/MWCNT-CP	4 nM	10^{-8} to 10^{-6} M	15 min	Zamfir et al. (2011)
AChE/MWCNTs-SnO_2-CHIT/SPE	$0.05–1.0\times10^{5}$ μg/L	0.05 μg/L	–	Chen et al. (2015)
FTO-AuNPs-chlAb	10 fM	1 fM to 1 μM	30 s	present work

(DPV) (Fig. 2A(ii)). Both results were in line with each other.

3.4. Optimization of various parameters of FTO-AuNPs-chl-Ab

To obtain the first-rate analytical performance of FTO-AuNPs electrode, the concentration of chl-Ab was optimized (Fig. 3A). The effect of response time of immobilized chl-Ab and chl-Ag was evaluated. The peak current increased up to 30 s and the current response decreased gradually after 35 s because enough chl-Ag attached to chl-Ab. Therefore, optimum response time observed was 30 s for efficient binding of chl-Ag to its specific Ab (Fig. 3B). The effect of temperature was also studied in order to maximize the current signal. The response current was increased at RT and decreased at 4 °C. Therefore, 25 °C was chosen as optimum temperature for subsequent studies (Fig. 3C). The FTO electrode was also optimized at various pH range from 6.0 to 8.0 as shown in Fig. 3D. The maximum current signal was observed at pH 7.5 that were used in binding and cross reactivity studies for further analysis in standard and real samples.

CV was recorded for FTO-AuNPs-chl-Ab at different scan rate (10–100 mV/s) in the presence of chl-Ag. Well defined anodic and cathodic peaks were observed for chl-Ag (Fig. 3E(i)). The magnitude of peak current is directly related to increase in the scan rate. The calibration curve was plotted (Fig. 3E(ii)) and values of the slope, intercept and correlation coefficient are given in the equations below. The dependency of the peak current (I) on the square root of the scan rate at 100 mV/scan be expressed as-

$$\text{Intercept} = -5.616\times10^{-4} \pm 6.608\times10^{-5}$$
$$\text{Slope} = 0.0011 \pm 4.570\times10^{-5}$$
$$Y = 0.0011\times + -5.616\times10^{-4}\ (r^2 = 0.98)$$

3.5. Analytical performance of FTO-AuNPs-chl-Ab nanosensor

The chl-Ag was detected by CV (Fig. 4A(i)) and DPV (Fig. 4B(i)) under optimum conditions. The peak current increased with increasing concentrations of chl-Ag, and a good linear relationship was established between current and the logarithm of chl-Ag concentration ranged from 1 fM to 1 μM. The linear regression equation for CV and for DPV were described in (Fig. 4A(ii)) and (Fig. 4B(ii)). For cyclic voltammetry (CV) the Intercept value was $4.404\times10^{-4} \pm 1.212\times10^{-5}$ and Slope was $1.121\times10^{-5} \pm 1.554\times10^{-6}$, hence the equation was $I = 1.12\times10^{-5}\times + 4.40\times10^{-4}$ (I(μA)) with $r^2 = 0.95$. For differential pulse voltammetry (DPV), the Intercept and slope was $4.245\times10^{-4} \pm 5.315\times10^{-6}$ and $2.514\times10^{-5} \pm 9.598\times10^{-7}$ with equation $I = 2.514\times10^{-5}\times + 4.245\times10^{-4}$ (I (μA)) and $r^2 = 0.98$; where, I = peak current; c = concentration of chl-Ag. The detection range and limit of detection (LOD) in standard samples was found to be 10 fM to 1 μM, and 10 fM respectively. The developed FTO-AuNPs-chl-Ab nanosensor reflected high sensitivity and improved signal amplification due to high conductance provided by AuNPs.

3.6. Cross-reactivity studies

The cross reactivity studies of FTO-AuNPs-chl-Ab nanosensor was performed with 2,4-D at linear range of concentration from 1 fM to 1 μM. 2,4-D is non-specific antigen therefore we observed negligible change in peak current (Fig. 4C-i). 2,4-D antigen were used as negative control (as 2,4-D is non-specific and does not bind with chl-Ab) and Chl-Ag as positive control due to its specificity for chlorpyrifos. Binding experiment was also conducted under same conditions with FTO-AuNPs-chl-Ab and chl-Ag. Addition of chl-Ag leads to dramatical increase in current response. The results indicated that the fabricated electrode system recognized chl-Ag with high degree of sensitivity and specificity with LOD up to 10 fM. Table 1 showed the comparative studies of the electrochemical sensors developed so far for the detection of chlorpyrifos. Furthermore, stability and regeneration studies were also done for FTO-AuNPs-chl-Ab fabricated electrode. For this, five sets of electrodes were fabricated for stability response over time and showed consistent results (Fig. 4C-ii). The repeatability of the proposed immunosensor was recorded on 7th, 14th, and 21st day of its fabrication on the same electrode and DPV response was monitored at 100 fM of chlorpyrifos (Fig. S1). The fabricated electrode system was kept at 4 °C upto 21 days and showed no difference in peak current while after 20 days the peak current decreased minimally that reconfirmed the better stability of nanosensor.

3.7. Application of FTO-AuNPs-chl-Ab nanosensor

The prepared biosensor was also tested in real samples such as apple, pomegranate and cabbage. The presence of pesticides in real samples was compared with the standard curve plotted at linear range from 1 fM to 1 μM (Fig. 4A and B). The FTO-AuNPs-chl-Ab nanosensor was able to detect chlorpyrifos up to 10 nM for apple, cabbage and 50 nM for pomegranate respectively (Fig. 4C (i)). We also analyzed the effect of food matrices on the detection limit of developed assay (Fig. S2). For this, the current response of chlorpyrifos antigen alone at 10 nM and 50 nM, and in food matrices was recorded. The current response was almost similar that could be easily depicted from Fig. S2. From the above observation, the developed sensor were not affected by food matrices. The obtained data predicted that the FTO-AuNPs-chl-Ab nanosensor can be used successfully for pesticide analysis in various other fruits and vegetables.

4. Conclusions

This study reports the development of an ultrasensitive FTO-AuNPs based nanosensor for the quantitative detection of chlorpyrifos in real samples such as fruits and vegetables upto 10 nM for apple and cabbage and 50 nM in pomegranate respectively. The present biosensor overcomes the limitations of sensitivity and specificity associated with earlier developed biosensor. In earlier developed biosensor, usage of enzyme affects the sensitivity and specificity because enzymes are very

sensitive towards change in experimental variables while antibodies are less affected by the experimental variable. Furthermore, coupling of smart elements such as gold nanoparticles and FTO provides better sensing platform which cause significant improvement in the detection range of pesticide. However, the utilization of sensing elements such as nanoparticles and antibody is slightly more as compared to other immunodiagnostic platforms. The linear range of the sensor was from 1 fM to 1 μM with LOD upto 10 fM. The nanosensor developed has potential application for chlorpyrifos detection. Combining the characteristics of FTO and AuNPs, a novel nanosensor exhibited many advantages such as fast response, highly sensitive, stable, simple fabrication and low cost. This work in future can be extended for detection of all types of pesticides on more economical substrates in one multiplexed system.

Acknowledgement

We greatly acknowledge the research grant DST/ECR/2016/000075 from Department of Science and Technology (DST), New Delhi, India for providing support to carry out the research work. Sergei A. Eremin acknowledges the support by Ministry of Education and Science of the Russian Federation, RFMEFI60417X0198.

Appendix A. Supporting information

Supplementary data associated with this article can be found in the online version at http://dx.doi.org/10.1016/j.bios.2018.01.013.

References

Alamgir Zaman Chowdhury, M., et al., 2013. Food Control 34, 457–465.
Azab, H.A., Anwar, Z.M., Rizk, M.A., Khairy, G.M., El-Asfoury, M.H., 2015. J. Lumin. 157, 371–382.
Chen, D., Jiao, Y., Jia, H., Guo, Y., Sun, X., Wang, X., Xu, J., 2015. Int. J. Electrochem. Sci. 10, 10491–10501.
Ding, J., Sun, X., Guo, Y., Jia, H., Qiao, L., Wang, X., 2014. J. Sens. Transducers 172, 27–33.
Frens, G., 1973. Nat. Phys. Sci. 241, 20–22.
Funari, R., Della Ventura, B., Schiavo, L., Esposito, R., Altucci, C., Velotta, R., 2013. Anal. Chem. 85, 6392–6397.
Funari, R., Della, B.V., Carrieri, R., Morra, L., Lahoz, E., Gesuele, F., Altucci, C., Velotta, R., 2015. Biosens. Bioelectron. 67, 224–229.
Gandhi, S., Caplash, N., Sharma, P., Suri, C.R., 2009. Biosens. Bioelectron. 25, 502–505.
Guan, H., Brewer, W.E., Garris, S.T., Morgan, S.L., 2010. J. Chromatogr. A 1217, 1867–1874.
Guohua, H., Hongyang, L., Zhiming, J., Danhua, Z., Haifang, W., 2017. Biosens. Bioelectron. 97, 184–195.
Hercegova, A., Domotorova, M., Matisova, E., 2007. J. Chromatogr. A 1153, 54–73.
Huang, X., Li, Y., Zhong, X., 2014. Nanoscale Res. Lett. 9, 572–576.
Hui, G., Zhang, J., Li, J., Zheng, L., 2016. Food Chem. 197, 1168–1176 (Pt B).
Hui, G., Jin, J., Deng, S., Ye, X., Zhao, M., Wang, M., Ye, D., 2015. Food Chem. 170, 484–491.
Jiao, Y., Jia, H., Guo, Y., Zhang, H., Wang, Z., Sun, X., Zhao, J., 2016. RSC Adv. 6, 58541–58548.
Jiaojiao, J., Yangyang, G., Gangying, Z., Yanping, C., Wei, L., Guohua, H., 2015. Food Chem. 15, 485–493.
Ji, D., Liu, L., Li, S., Chen, C., Lu, Y., Wu, J., Liu, Q., 2017. Biosens. Bioelectron. 15, 449–456.
Li, Y.R., Gan, Z.Y., Li, Y.F., Liu, Q., Bao, J.C., Dai, Z.H., Han, M., 2010. Sci. China Chem. 53, 820–825.
Li, J., Zheng, F., Jiang, J., Lina, H., Hui, G., 2015. Anal. Methods 7, 9928–9939.
Luo, Y.L., Xu, J.Y., Li, Y., Gao, H.T., Guo, J.J., Shen, F., Sun, C.Y., 2015. Food Control. 54, 7–15.
Lu, Y., Huang, Y., Li, S., Zhang, Q., Wu, J., Xiong, Z., Xiong, L., Wan, Q., Liu, Q., 2017. Sens. Actuators B: Chem. 252, 973–982.
Moraes, F.C., Mascaro, L.H., Machado, S.A., Brett, C.M., 2009. Talanta 79, 1406–1411.
Nunes, G.S., Jeanty, G., Marty, J.L., 2004. Anal. Chim. Acta 523, 107–115.
Qu, Y., Sun, Q., Xiao, F., Shi, G., Jin, L., 2010. Bioelectrochemistry 77, 139–144.
Seiber, J.N., Kleinschmidt, L.A., 2011. J. Agric. Food Chem. 59, 7536–7543.
Sharma, P., Gandhi, S., Chopra, A., Sekar, N., Suri, C.R., 2010. Anal. Chim. Acta 676, 87–92.
Song, Y.H., Zhang, M., Wang, L., Wan, L.L., Xiao, X.P., Ye, S.H., Wang, J.G., 2011. Electrochim. Act. 56, 7267–7271.
Suri, C.R., Boro, R., Nangia, Y., Gandhi, S., Sharma, P., Wangoo, N., Rajesh, K., Shekhawat, G.S., 2009. Trends Anal. Chem. 28, 29–39.
Sun, X., Cao, Y., Gong, Z., Wang, X., Zhang, Y., Gao, J., 2012a. Sensors 12, 17247–17261.
Sun, X., Cao, Y., Gong, Z., Wang, X., Zhang, Y., Gao, J., 2012b. Sensors 12, 17247–17261.
Suri, C.R., Kaur, J., Gandhi, S., Shekhawat, G.S., 2008. Nanotechnol 19, 235502.
Tang, T.T., Deng, J.J., Zhang, M., Shi, G.Y., Zhou, T.S., 2016. Talanta 146, 55–61.
Tey, J.N., Gandhi, S., Wijaya, I.P.M., Palaniappan, Al, Wei, J., Rodriguez, I., Suri, C.R., Mhaisalkar, S.G., 2010. Small 6, 993–998.
Thakur, S., Gandhi, S., Paul, A.K., Suri, C.R., 2011. Sens. Transd 131, 91–100.
Viswanathan, S., Radecka, H., Radecki, J., 2009. Biosens. Bioelectron. 24, 2772–2777.
Wang, k., Liu, Q., Yan, J.J., Ju, C., Qiu, B.J., Wu, X.Y., 2011. Anal. Chim. Acta 695, 84.
Wijaya, I.P.M., Tey, J.N., Gandhi, S., Boro, R., Palaniappan, Al, Hau, G.W., Rodriguez, I., Suri, C.R., Mhaisalkar, S.G., 2010. Lab Chip 5, 634–638.
Xiang, L., Tang, J.S., 2017. RSC Adv. 7, 8332–8337.
Zamfir, L.G., Rotariu, L., Bala, C., 2011. Biosens. Bioelectron. 26, 3692–3695.
Zalat, O.A., Elsayed, M.A., Fayed, M.S., Abd El Megid, M.K., 2014. Int. Lett. Chem. Phys. Astron. 2, 58–63.
Zhao, X.S., Kong, W.J., Wei, J.H., Yang, M.H., 2014. Food Chem. 162, 270–276.
Zhang, X., Zhao, Z., Lou, X., Li, J., Hui, G., 2017. J. Food Meas. Charact. 11, 548–555.
Zhu, J., 2015. Bioeng 6, 283–287.